HHS Public Access

Author manuscript

Nat Struct Mol Biol. Author manuscript; available in PMC 2012 December 01.

Published in final edited form as:

Nat Struct Mol Biol. ; 19(6): 616–622. doi:10.1038/nsmb.2288.

Dynamic and static components power unfolding in topologically closed rings of a AAA+ proteolytic machine

Steven E. Glynn[1], **Andrew R. Nager**[1], **Tania A. Baker**[1,2], and **Robert T. Sauer**[1]

[1]Department of Biology, Massachusetts Institute of Technology, Cambridge, Massachusetts 02139 USA

[2]Howard Hughes Medical Institute, Massachusetts Institute of Technology, Cambridge, Massachusetts 02139 USA

Abstract

In the *E. coli* ClpXP protease, a hexameric ClpX ring couples ATP binding and hydrolysis to mechanical protein unfolding and translocation into the ClpP degradation chamber. Rigid-body packing between the small AAA+ domain of each ClpX subunit and the large AAA+ domain of its neighbor stabilizes the hexamer. By connecting the parts of each rigid-body unit with disulfide bonds or linkers, we created covalently closed rings that retained robust activity. A single-residue insertion in the hinge that connects the large and small AAA+ domains and forms part of the nucleotide-binding site uncoupled ATP hydrolysis from productive unfolding. We propose that ATP hydrolysis drives changes in the conformation of one hinge and its flanking domains, which are propagated around the AAA+ ring via the topologically constrained set of rigid-body units and hinges to produce coupled ring motions that power substrate unfolding.

Mechanical force is used to drive vectorial work in many cellular processes. In organisms from bacteria to humans, molecular machines of the AAA+ family (ATPases Associated with various cellular Activities) couple energy derived from ATP binding and hydrolysis to the degradation, remodeling, or movement of macromolecules[1,2]. These enzymes work as protein unfoldases, disaggregating machines, DNA and RNA helicases, macromolecular pumps, and microtubule motor and severing proteins. How these machines function is an active area of investigation.

Escherichia coli ClpX is a hexameric AAA+ machine that unfolds protein substrates and translocates them into the degradation chamber of ClpP, a self-compartmentalized peptidase[3] (Fig. 1A). Crystal structures of ClpX have been solved in a open helical conformation and as a ring hexamer[4,5]. Lock-washer and helical conformations of some AAA+ machines are thought to be the relevant species for biological function[6–10]. For ClpX, present evidence supports a functional role for the ring conformation, but it is unclear

Address correspondence to bobsauer@mit.edu.

Author contributions. S.E.G. and A.R.N. performed all experiments. S.E.G., A.R.N., T.A.B. and R.T.S. contributed to experimental design, interpretation, and writing the manuscript.

if the ring opens during the conformational fluctuations that power protein unfolding or when multiple polypeptides need to be translocated during the degradation of disulfide-bonded substrates[3]. Another aspect of understanding ClpX function is determining which structural elements provide the flexibility to adopt the different conformations needed for machine function, while maintaining a sufficiently rigid overall structure to apply the forces needed to unfold native proteins. Macroscopic machines typically consist of rigid components that are flexibly linked to allow them to move with respect to each other. For example, the pistons of an internal combustion engine connect to the crankshaft in a way that allows piston movement to rotate the crankshaft, which can then be coupled to many different kinds of mechanical work.

The AAA+ module of ClpX consists of a large domain (residues 65–314), a short hinge (residues 315–318), and a small domain (residues 319–424)[4,11–12]. In ring hexamers, the small AAA+ domains are on the periphery of the ring, whereas the large AAA+ domains surround an axial pore, which is lined by loops that help the enzyme grip and translocate substrates[5,13–17] (Fig. 1B). Although ClpX subunits are identical in sequence, they adopt distinct conformations and roles during the ATPase cycle[5,15–16,18]. In four loadable subunits, a cleft between the large and small AAA+ domains provides a binding site for ATP or ADP, with nucleotide contacts made by each domain and by the intervening hinge (Fig. 1C); these subunits display a range of nucleotide-binding properties and modest changes in the nucleotide-dependent conformation of the hinge[5,18]. Two opposed unloadable subunits in the ClpX ring do not bind nucleotide, because a radically different hinge conformation rotates the large and small AAA+ domains enough to destroy the binding cleft. Despite inherent asymmetry of the ring, each large AAA+ domain packs against the small AAA+ domain of the neighboring subunit in a nearly invariant manner[5] (Fig. 1D, 1E). A static ring can therefore be viewed as six rigid-body units, each spanning two subunits, connected by six hinges (Fig. 1D).

Here, we ask if a ClpX hexamer functions as a closed ring and if the rigid-body packing between subunits is preserved throughout all of the different conformational changes that define the ATP-fueled mechanical cycle. Specifically, we engineer and assay the functional effects of covalent ties that tightly restrict the rigid-body packing between neighboring large and small domains in hexamers. Strikingly, mutants constrained in this fashion have a topologically closed ring but mediate robust unfolding and degradation. These results in combination with the properties of a hinge mutant strongly support a model in which conformational changes, which originate in one hinge and its flanking domains as a consequence of ATP binding or hydrolysis, are propagated around the AAA+ ring via the topologically constrained set of rigid-body units and hinges, producing coupled ring motions that power substrate unfolding.

Results

Tight subunit-subunit tethering does not affect activity

For the studies described below, we used $ClpX^{\Delta N}$ variants that contain the complete AAA+ module but lack a family-specific N-terminal domain. $ClpX^{\Delta N}$ is active in ClpP-mediated degradation of protein substrates bearing an ssrA degradation tag at the C terminus[11–12,15].

Previous studies showed that the N- and C-termini of adjacent ClpX$^{\Delta N}$ subunits, which span the rigid-body interface between subunits, could be connected by 20-residue peptide tethers (T_{20}) with retention of full ATP-dependent unfolding and degradation activity in pseudo hexamers composed of single-chain dimers, trimers, or hexamers[15,19]. By covalently connecting the small AAA+ domain of one subunit to the large AAA+ domain of the next subunit, these peptide tethers fuse both elements of the rigid-body unit.

To probe the importance of tether length and limit potential motions between the small and large domains of single rigid-body units, we constructed single-chain trimers with three ClpX$^{\Delta N}$ subunits connected by tethers of four (T_4) or zero (T_0) residues for comparison with the T_{20} single-chain trimer. Fig. 2A depicts the structural elements in these single-chain trimers, which include two complete rigid-body units; Fig. 2B shows two single-chain trimers in the context of a pseudo hexamer. Like the T_{20} enzyme, the T_4 and T_0 variants purified predominantly as pseudo-hexamers during gel-filtration chromatography (Fig. 2C). Irrespective of tether length, each variant had a similar basal ATP-hydrolysis activity (Fig. 2D). Moreover, these ATPase activities were all repressed modestly in the presence of ClpP and were all enhanced ~3-fold in the presence of an unfolded protein substrate (carboxymethylated-titin^{I27}-ssrA; ref. 20; Fig. 2D). Importantly, each single-chain trimer supported comparable rates of ClpP-mediated degradation of a GFP-ssrA substrate over a 40-fold range of substrate concentrations (Fig. 2E), and fitting of these data yielded similar K_M and V_{max} values (Table 1). ClpX unfolding of GFP-ssrA, which is a thermodynamically and kinetically stable protein, is the rate-limiting step in proteolysis[21]. Moreover, ClpXP degradation of this substrate requires highly coordinated unfolding and translocation driven by a high rate of ATP hydrolysis[22–23]. We conclude that the T_4 and T_0 tethers are compatible with all of the different conformational states adopted by ClpX during the machine cycles that drive substrate unfolding and translocation into ClpP.

The N- and C-terminal residues of adjacent ClpX$^{\Delta N}$ subunits (residues 61–423) are directly fused in the T_0-linked ClpX$^{\Delta N}$ single-chain trimer. In the crystal structure of the nucleotide-bound ClpX$^{\Delta N}$ hexamer (pdb code 3HWS)[5], the last ordered C-terminal position of each subunit (residues 413–415) was ~24 Å from the first ordered N-terminal position of the next subunit (residues 62–63). The ~10 residues missing in the crystal structure would be sufficient to span this gap between subunits in the T_0 ClpX$^{\Delta N}$ singe-chain trimer, but the linkage would be predicted to be tight and thus to substantially constrain movement of the parts of the rigid-body unit.

Covalently closed ClpX rings are fully functional

As an additional method of limiting movement within the rigid-body units, we searched the crystal structure of the ClpX hexamer to identify pairs of residues where disulfide bonds could covalently connect the small and large domains of adjacent subunits. Two solutions with good geometry were found, one corresponding to substituting cysteines for ClpX residues Thr66 and Pro388 and one substituting cysteines for Glu109 and Asn331. We initially constructed a T_{20} single-chain dimer with the T66C substitution in the large AAA+ domain of the N-terminal ClpX$^{\Delta N}$ subunit and the P388C substitution in the small AAA+ domain of the C-terminal subunit (Fig. 3A). Association of three of these dimers in a

pseudo-hexamer should permit formation of three native disulfide bonds (Fig. 3B). Immediately following purification, non-reducing SDS-PAGE showed a (T66C P388)–(T66 P388C) species corresponding to the reduced single-chain dimer (~80 kDa), as well as smaller amounts of disulfide-linked tetramers (~160 kDa), and disulfide-linked hexamers (~240 kDa; Fig. 3C, lane 2). After catalyzing oxidation by addition of copper phenanthroline, we observed time-dependent changes in the concentrations of three disulfide-bonded species (Fig. 3C). The apparent molecular weights and kinetics of appearance and disappearance of these species allowed their assignment as disulfide-bonded linear tetramers, disulfide-bonded linear hexamers, and disulfide-bonded circular hexamers, respectively. These assignments were confirmed by following the kinetics of reduction by dithiothreitol, which showed that the circular hexamer chased into the linear hexamer, which formed the linear tetramer, which was reduced to the linked dimer (Fig. 3D). Importantly, after oxidation 90–95% of the protein was present as the disulfide-bonded circular hexamer. A small fraction remained as dimers or linear tetramers or hexamers, presumably because of competing cysteine modifications that prevent complete disulfide-bond formation.

We also constructed and purified a T_{20}-linked dimer with the E109C mutation in the first $ClpX^{\Delta N}$ subunit and the N331C mutation substitution in the second subunit (E109C N331)—(E109 N331C). This protein formed the disulfide-bonded circular hexamer in ~90% yield following incubation with copper phenanthroline (Fig. 3E).

In the disulfide-bonded circular hexamers consisting of (T66C P388)—(T66 P388C) or (E109C N331)—(E109 N331C) single-chain dimers, every subunit is covalently connected to both flanking subunits, either by a disulfide bond that fuses a rigid-body unit or by a T_{20} tether (Fig. 3B). Both classes of disulfide-bonded circular hexamers hydrolyzed ATP at least as well as the reduced enzymes (Table 1). More importantly, both disulfide-bonded enzymes supported ClpP-dependent degradation of GFP-ssrA with steady-state rates and kinetic parameters essentially identical to the pseudo hexamer formed by wild-type single-chain dimers (Fig. 3F; Table 1). We conclude that hexameric rings that are topologically closed by covalent linkage can perform all of the normal machine functions of ClpX, including ATP hydrolysis, recognition, unfolding, processive translocation of GFP-ssrA (a ~28 kDa substrate), and association and cooperation with ClpP during protein degradation.

Constraining rigid-body units with disulfide bonds

Next, we constructed and purified a hexamer composed of six untethered $ClpX^{\Delta N}$ subunits containing the T66C and P388C substitutions. Following purification, non-reducing SDS-PAGE revealed species corresponding to monomers as well as disulfide-bonded dimers, trimers, tetramers, pentamers, and linear hexamers. Oxidation catalyzed by copper phenanthroline converted ~75% of the protein into the disulfide-bonded circular hexamer (Fig. 4A), a species with disulfide-bonds connecting the two elements of each rigid-body unit. The ~3:1 mixture of disulfide-bonded circular and linear hexamers supported ClpP degradation of GFP-ssrA at rates only slightly lower than those of the $ClpX^{\Delta N}$ parental enzyme (Fig. 4B; Table 1), supporting a model in which the disulfide bonds that lock each rigid-body unit in the hexameric ring are compatible with ClpX function. By contrast, when we fully reduced the T66C P388C enzyme by incubation with dithiothreitol, V_{max} for

degradation of GFP-ssrA decreased ~4-fold and K_M increased ~20-fold in comparison to the oxidized enzyme (Fig. 4B; Table 1). This result suggests that the T66C and/or P388C mutations destabilize the interfaces between the parts of each rigid-body unit, resulting in slower unfolding and degradation, whereas formation of the disulfide bonds stabilizes these interfaces.

To constrain possible movements of the interfaces within rigid-body units further, we also constructed and purified a ClpX$^{\Delta N}$ variant containing the T66C, E109C, N331C, and P388C mutations, allowing formation of two disulfide bonds within each of the six rigid-body units. The purified enzyme again contained monomers and disulfide-bonded dimers, trimers, tetramers, pentamers, and linear hexamers, but oxidation converted >90% of the protein into a circular hexamer (Fig. 4C). The oxidized T66C P388C E109C N331C enzyme supported ClpP degradation of GFP-ssrA with a V_{max} ~30% of that of ClpX$^{\Delta N}$ (Fig. 4D; Table 1). We also tested proteolysis of cp7-GFP-ssrA, a circularly permuted GFP variant that is easier for ClpXP to unfold[23], which was degraded with a V_{max} ~70% of that of the ClpX$^{\Delta N}$ enzyme (Fig. 4D; Table 1). Following reduction of the T66C P388C E109C N331C protein, by contrast, the rate of ATP hydrolysis was ~15-fold lower (Table 1) and the protein did not support ClpP-mediated degradation of GFP-ssrA or cp7-GFP-ssrA (not shown).

ClpP enhances unfolding by covalently closed ClpX hexamers

The protein-unfolding activity of ClpX is enhanced in the ClpXP complex[19,21]. This observation might be explained if ClpP binding stabilizes the rigid-body interactions between ClpX subunits and prevents opening of the ClpX ring. If this were the only mechanism by which ClpP affected unfolding, however, then ClpP binding would not be expected to enhance the unfolding activity of ClpX variants in which the subunit-subunit interfaces were already stabilized by disulfide bonding. To test this possibility, we devised an assay to monitor protein unfolding by ClpX in the absence of ClpP. The fluorescent protein Kaede undergoes photo-cleavage at a single site following exposure to UV light, which also changes the fluorescent properties of the native protein[24]. We appended an ssrA tag to Kaede and found that photo-cleavage prevented refolding following denaturation, allowing unfolding of cleaved Kaede-ssrA by ClpX variants to be monitored by loss of native fluorescence (Fig. 5A).

As shown in Fig. 5B, ClpX$^{\Delta N}$ unfolded the cleaved Kaede-ssrA substrate ~2.5-fold more rapidly in the presence than absence of ClpP. However, ClpP also enhanced the rate at which the singly (T66C P388C) and doubly (T66C P388C E109C N331C) disulfide-bonded variants of ClpX$^{\Delta N}$ unfolded Kaede-ssrA (Fig. 5B). These results suggest that ClpP enhancement of ClpX unfolding is not mediated solely by stabilization of the closed ClpX ring.

Translocation of multiple polypeptides by closed ClpX rings

Concurrent translocation of two or three polypeptide chains through the axial pore of ClpX is required when ClpXP initiates degradation at internal sites or degrades disulfide-bonded substrates[25–27] (Fig. 5C). Compared to normal translocation, this activity almost certainly requires substantial pore expansion, which might be accomplished by ClpX-ring opening. If

so, then covalently constraining the subunit-subunit interfaces would prevent degradation of disulfide-bonded substrates. To test this possibility, we assayed degradation of a disulfide-bonded variant of the N11C-Arc-ssrA dimer by SDS-PAGE[25]. Notably, ClpX$^{\Delta N}$ and a enzyme mixture with >90% disulfide-bonded circular hexamers of T66C P388C E109C N331C ClpX$^{\Delta N}$ supported ClpP-mediated degradation of this cross-linked substrate equally well (Fig. 5D). We conclude that ClpX unfolding and translocation of multiple polypeptide chains does not require ring opening or other major distortions of the rigid-body packing units that form the major interface between subunits.

Hinge mutations uncouple ATP hydrolysis from unfolding

Our results indicate that the rigid-body units of the ClpX hexamer remain intact during ATP hydrolysis and the coupled processes of substrate unfolding and translocation, leaving the hinges between domains as the likely source of the nucleotide-dependent rearrangements that allow the ring to change conformation. Fig. 6A shows that the length of the ClpX hinge is conserved in orthologs, suggesting that changes in hinge length could be detrimental to function.

To test this hypothesis, we deleted Asn315 in the hinge (Δ315N) or duplicated this residue (+315N), purified these variants, and assayed their activities. Asn315 was chosen as the hinge residue to mutate because it shows the greatest conformation variation in backbone dihedral angles in different ClpX subunits[5]. Both mutants purified as hexamers (not shown) and retained substantial ATP-hydrolysis activity in the presence and absence of substrate (Fig. 6B). In protein degradation assays with ClpP, Δ315N ClpX$^{\Delta N}$ had ~10% of the wild-type V_{max} in degrading GFP-ssrA (Fig. 6C) and ~70% of wild-type activity in degrading cp7-GFP (Fig. 6D). Importantly, however, the +315N variant displayed very low levels of degradation of GFP-ssrA or the less stable cp7-GFP substrate (Fig. 6C, 6D). In principle, this severely reduced degradation activity of the +315N enzyme could arise from defects in substrate recognition, unfolding, translocation, and/or interaction with ClpP. We found, however, that +315N ClpX$^{\Delta N}$–ClpP degraded carboxymethylated-titin^{I27}-ssrA at ~20% of the rate of ClpX$^{\Delta N}$–ClpP (Fig. 6E). Proteolysis of this unfolded protein requires recognition and translocation of the substrate into ClpP[20,28]. Thus, inserting one residue in the ClpX hinge did not prevent ATP hydrolysis, substrate binding, or ClpP recognition but severely reduced protein-unfolding activity and also slowed translocation. These results support a critical role for the hinge in allowing ClpX to carry out these mechanical processes.

Discussion

Cellular machines use an energy source, typically NTP hydrolysis or a proton gradient, to power a sequence of conformational changes that can be coupled to mechanical work. Thus, an important challenge in deciphering molecular mechanism is determining which macromolecular conformations participate in the functional machine cycle. Crystal structures provide a snapshot of accessible three-dimensional conformations, but biochemical studies are needed to determine if these structures are functionally relevant. In the case of ClpX, crystals structures have shown that subunits can interact to form open structures with helical symmetry or closed hexameric rings that are fundamentally

asymmetric[4–5]. In the work presented here, we have engineered ClpX variants in which the hexameric ring is topologically closed. Importantly, these rings hydrolyze ATP, recognize protein substrates, unfold and translocate these molecules (even when translocation of multiple polypeptide chains is required), and interact productively with ClpP to carry out energy-dependent protein degradation. In combination, these studies provide strong evidence that open-ring ClpX structures are not required for basic machine function nor for protein unfolding and processive translocation and degradation, which can require hundreds of cycles of ATP hydrolysis and coupled conformational changes in the ring[20,29].

Rigid-body subunit contacts limit functional conformations

Except for differences in loops and side-chain conformations, the three-dimensional structures of the large and small AAA+ domains of ClpX show little variation in different crystal structures and are also highly conserved in structures of the paralogous HslU, ClpA, FtsH, Lon, and ClpC enzymes[4–5,30–36]. Moreover, although crystallographic ClpX rings are asymmetric, the small AAA+ domain of every subunit packs against the large AAA+ domain of the neighboring subunit in a very similar rigid-body manner[5] (Fig. 1D, 1E). Indeed, we find that different covalent constraints across this subunit-subunit interface are compatible with ClpX function, demonstrating that the enzyme can adopt all of the different conformational states that comprise the functional reaction cycle without breaking or substantial distortion of the crystallographically observed rigid-body interfaces between subunits. These observations strongly support a model in which the rigid-body units undergo very little motion as ATP binding and hydrolysis drive ClpX through the different conformations needed to unfold and translocate protein substrates.

The hinge connecting ClpX domains plays an important role

If the six rigid-body units in an *E. coli* ClpX ring remain largely structurally invariant, as our results indicate, then conformational changes in the hinge (residues 315–318), which links the large and small AAA+ domains of each subunit (Fig. 6A), are likely to mediate the nucleotide-dependent ring motions required for generating the mechanical work of protein unfolding and translocation. Indeed, we find that inserting a single residue in the ClpX hinge uncouples ATP hydrolysis from robust protein unfolding. ATP and ADP bind in clefts between the large and small AAA+ domains of the four loadable ClpX subunits[5] (Fig. 6A), with nucleotide contacts made by both AAA+ domains and one hinge side chain (Leu317 in *E. coli* ClpX). Hence, nucleotide binding, hydrolysis, and dissociation could easily result in changes in the orientations of the large domain, hinge, and small domain in a single subunit. These structural changes would then be propagated to the immediate flanking subunits via the rigid-body units, which would alter the next set of subunits, and so on. Moreover, because the ClpX ring remains topologically closed during function, the backbone torsion angles of the hinge residues in every subunit would be constrained to combinations compatible with ring closure. ATP hydrolysis in a single ClpX subunit is known to be able to power protein unfolding and translocation[15]. Topological closure and the conservation of rigid-body packing units would allow nucleotide-dependent changes initiated by ATP binding or hydrolysis in a single subunit to change the conformation of the entire ring in a concerted fashion.

Force generation requires a stable subunit interface

Previous studies revealed that ClpX mutants with substitutions in the rigid-body interface between neighboring subunits (L381K; D382K; Y385A) were competent to hydrolyze ATP and bind ssrA-tagged substrates but could not unfold protein substrates unless ClpP was also present[37–38]. These results suggest that ClpP binding helps to stabilize the rigid-body interfaces between subunits in a ClpX ring and imply that the integrity of these interfaces is required for the efficient generation of mechanical force, perhaps by preventing substrate slipping during translocation-induced unfolding. In the current studies, we found that the reduced form of the T66C P388C ClpX$^{\Delta N}$ variant supported ClpP-mediated degradation of GFP-ssrA with a maximum velocity ~4-fold lower than the same enzyme after formation of disulfide bonds across the rigid-body subunit interfaces. Because protein unfolding is the rate-limiting step in GFP-ssrA degradation by ClpXP[21], the T66C and/or P388C mutations must reduce the unfolding activity of the reduced enzyme, most likely by destabilizing the rigid-body interfaces between subunits. Even more dramatically, the reduced variant containing the T66C, E109C, N331C, and P388C mutations was inactive in protein unfolding and degradation, but these activities were restored when the rigid-body interface between subunits was stabilized by disulfide-bond formation.

The work presented here reveals that ClpX functions as a closed hexameric ring with critical subunit-subunit contacts established by rigid-body packing between the large and small AAA+ domains of neighboring subunits. Both the integrity of these rigid-body interfaces between subunits and the hinge sequences that link the six rigid-body units of the AAA+ ring play important functional roles in coupling ATP binding and hydrolysis to protein unfolding. It will be important to determine if these properties are shared by the AAA+ unfolding rings of other ATP-dependent proteases and disassembly chaperones, including Lon, FtsH, ClpAP, ClpCP, PAN–20S, the 26S proteasome, ClpB, and Hsp104.

Supplementary Material

Refer to Web version on PubMed Central for supplementary material.

Acknowledgments

This work was supported by NIH grant AI-15706 (R.T.S.). T.A.B. is an employee of the Howard Hughes Medical Institute. We thank B. Stinson and B. Sosa for help and discussions and P. Schwille (Dresden University of Technology) for providing the Kaede plasmid.

References

1. Hanson PI, Whiteheart SW. AAA+ proteins: have engines, will work. Nat Rev Mol Cell Biol. 2005; 6:519–529. [PubMed: 16072036]
2. White SR, Lauring B. AAA+ ATPases: achieving diversity of function with conserved machinery. Traffic. 2007; 8:1657–1667. [PubMed: 17897320]
3. Baker TA, Sauer RT. ClpXP, an ATP-powered unfolding and protein-degradation machine. Biochim Biophys Acta. 2012; 1823:15–28. [PubMed: 21736903]
4. Kim DY, Kim KK. Crystal structure of ClpX molecular chaperone from *Helicobacter pylori*. J Biol Chem. 2003; 278:50664–50670. [PubMed: 14514695]

5. Glynn SE, Martin A, Nager AR, Baker TA, Sauer RT. Structures of asymmetric ClpX hexamers reveal nucleotide-dependent motions in a AAA+ protein-unfolding machine. Cell. 2009; 139:744–756. [PubMed: 19914167]
6. Jeruzalmi D, O'Donnell M, Kuriyan J. Crystal structure of the processivity clamp loader gamma (gamma) complex of *E. coli* DNA polymerase III. Cell. 2001; 106:429–441. [PubMed: 11525729]
7. Skordalakes E, Berger JM. Structure of the Rho transcription terminator: mechanism of mRNA recognition and helicase loading. Cell. 2003; 114:135–146. [PubMed: 12859904]
8. Erzberger JP, Mott ML, Berger JM. Structural basis for ATP-dependent DnaA assembly and replication-origin remodeling. Nat Struct Mol Biol. 2006; 13:676–683. [PubMed: 16829961]
9. Mott ML, Erzberger JP, Coons MM, Berger JM. Structural synergy and molecular crosstalk between bacterial helicase loaders and replication initiators. Cell. 2008; 135:623–634. [PubMed: 19013274]
10. Simonetta KR, et al. The mechanism of ATP-dependent primer-template recognition by a clamp loader complex. Cell. 2009; 137:659–671. [PubMed: 19450514]
11. Singh SK, et al. Functional domains of the ClpA and ClpX molecular chaperones identified by limited proteolysis and deletion analysis. J Biol Chem. 2001; 276:29420–29429. [PubMed: 11346657]
12. Wojtyra UA, Thibault G, Tuite A, Houry WA. The N-terminal zinc binding domain of ClpX is a dimerization domain that modulates the chaperone function. J Biol Chem. 2003; 278:48981–48990. [PubMed: 12937164]
13. Ortega J, Lee HS, Maurizi MR, Steven AC. ClpA and ClpX ATPases bind simultaneously to opposite ends of ClpP peptidase to form active hybrid complexes. J Struc Biol. 2004; 146:217–226.
14. Siddiqui SM, Sauer RT, Baker TA. Role of the processing pore of the ClpX AAA+ ATPase in the recognition and engagement of specific protein substrates. Genes Dev. 2004; 18:369–374. [PubMed: 15004005]
15. Martin A, Baker TA, Sauer RT. Rebuilt AAA + motors reveal operating principles for ATP-fuelled machines. Nature. 2005; 437:1115–1120. [PubMed: 16237435]
16. Martin A, Baker TA, Sauer RT. Pore loops of the AAA+ ClpX machine grip substrates to drive translocation and unfolding. Nat Struct Mol Biol. 2008a; 15:1147–1151. [PubMed: 18931677]
17. Martin A, Baker TA, Sauer RT. Diverse pore loops of the AAA+ ClpX machine mediate unassisted and adaptor-dependent recognition of ssrA-tagged substrates. Mol Cell. 2008; 29:441–450. [PubMed: 18313382]
18. Hersch GL, Burton RE, Bolon DN, Baker TA, Sauer RT. Asymmetric interactions of ATP with the AAA+ ClpX6 unfoldase: allosteric control of a protein machine. Cell. 2005; 121:1017–1027. [PubMed: 15989952]
19. Martin A, Baker TA, Sauer RT. Distinct static and dynamic interactions control ATPase-peptidase communication in a AAA+ protease. Mol Cell. 2007; 27:41–52. [PubMed: 17612489]
20. Kenniston JA, Baker TA, Fernandez JM, Sauer RT. Linkage between ATP consumption and mechanical unfolding during the protein processing reactions of an AAA+ degradation machine. Cell. 2003; 114:511–520. [PubMed: 12941278]
21. Kim YI, Burton RE, Burton BM, Sauer RT, Baker TA. Dynamics of substrate denaturation and translocation by the ClpXP degradation machine. Mol Cell. 2000; 5:639–648. [PubMed: 10882100]
22. Martin A, Baker TA, Sauer RT. Protein unfolding by a AAA+ protease: critical dependence on ATP-hydrolysis rates and energy landscapes. Nat Struct Mol Biol. 2008; 15:139–145. [PubMed: 18223658]
23. Nager AR, Baker TA, Sauer RT. Stepwise unfolding of a β-barrel protein by the AAA+ ClpXP protease. J Mol Biol. 2011; 413:4–16. [PubMed: 21821046]
24. Ando R, Hama H, Yamamoto-Hino M, Mizuno H, Miyawaki A. An optical marker based on the UV-induced green-to-red photoconversion of a fluorescent protein. Proc Nat Acad Sci. 2002; 99:12651–12656. [PubMed: 12271129]

25. Burton RE, Siddiqui SM, Kim YI, Baker TA, Sauer RT. Effects of protein stability and structure on substrate processing by the ClpXP unfolding and degradation machine. EMBO J. 2001; 20:3093–3100.
26. Hoskins JR, Yanagihara K, Mizuuchi K, Wickner S. ClpAP and ClpXP degrade proteins with tags located in the interior of the primary sequence. Proc Natl Acad Sci USA. 2002; 99:11037–11042. [PubMed: 12177439]
27. Bolon DN, Grant RA, Baker TA, Sauer RT. Nucleotide-dependent substrate handoff from the SspB adaptor to the AAA+ ClpXP protease. Mol Cell. 2004; 16:343–350. [PubMed: 15525508]
28. Kenniston JA, Baker TA, Sauer RT. Partitioning between unfolding and release of native domains during ClpXP degradation determines substrate selectivity and partial processing. Proc Natl Acad Sci USA. 2005; 102:1390–1395. [PubMed: 15671177]
29. Aubin-Tam ME, Olivares AO, Sauer RT, Baker TA, Lang MJ. Single-molecule protein unfolding and translocation by an ATP-fueled proteolytic machine. Cell. 2011; 145:257–267. [PubMed: 21496645]
30. Bochtler M, et al. The structures of HslU and the ATP-dependent protease HslU-HsIV. Nature. 2000; 403:800–805. [PubMed: 10693812]
31. Sousa MC, et al. Crystal and solution structures of an HslUV protease-chaperone complex. Cell. 2000; 103:633–643. [PubMed: 11106733]
32. Guo F, Maurizi MR, Esser L, Xia D. Crystal structure of ClpA, an Hsp100 chaperone and regulator of ClpAP protease. J Biol Chem. 2002; 277:46743–46752. [PubMed: 12205096]
33. Krzywda S, et al. The crystal structure of the AAA domain of the ATP-dependent protease FtsH of *Escherichia coli* at 1.5 Å resolution. Structure. 2002; 10:1073–1783. [PubMed: 12176385]
34. Cha SS, et al. Crystal structure of Lon protease: molecular architecture of gated entry to a sequestered degradation chamber. EMBO J. 2010; 29:3520–3530. [PubMed: 20834233]
35. Duman RE, Löwe J. Crystal structures of *Bacillus subtilis* Lon protease. J Mol Biol. 2010; 401:653–670. [PubMed: 20600124]
36. Wang F, et al. Structure and mechanism of the hexameric MecA-ClpC molecular machine. Nature. 2011; 471:331–335. [PubMed: 21368759]
37. Joshi SA, Baker TA, Sauer RT. C-terminal domain mutations in ClpX uncouple substrate binding from an engagement step required for unfolding. Mol Micro. 2003; 48:67–76.
38. Joshi SA, Hersch GL, Baker TA, Sauer RT. Communication between ClpX and ClpP during substrate processing and degradation. Nat Struct Mol Biol. 2004; 11:404–411. [PubMed: 15064753]
39. Crooks GE, Hon G, Chandonia JM, Brenner SE. WebLogo: A sequence logo generator. Genome Res. 2004; 14:1188–1190. [PubMed: 15173120]

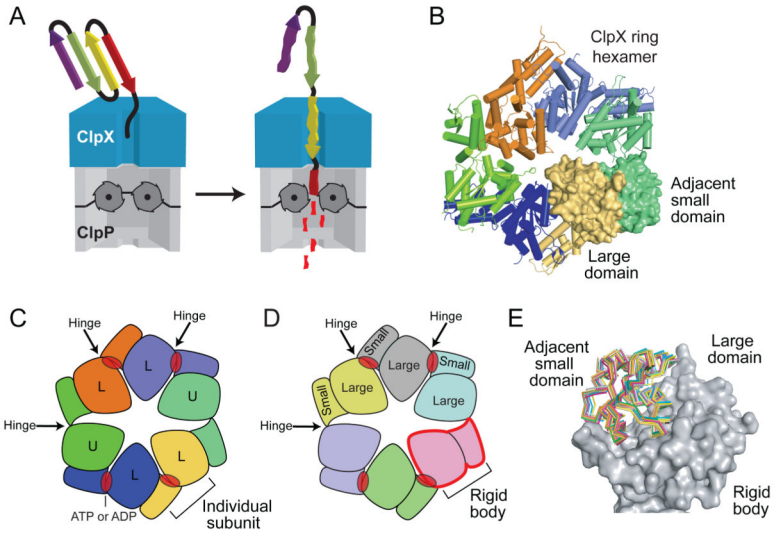

Figure 1.

The $ClpX_6$ ring is stabilized by rigid-body packing between subunits. (**a**) In the ATP-dependent ClpXP protease, a ClpX hexamer recognizes and unfolds protein substrates, and then translocates them into the degradation chamber of $ClpP_{14}$ for proteolysis. The unfolding and translocation reactions require ATP hydrolysis. **(b)** Crystal structure of a ring hexamer of $ClpX^{\Delta N}$ (pdb code 3HWS)[5]. Four subunits are shown in cartoon representation. The large AAA+ domain of one subunit (yellow; surface representation) packs against the small AAA+ domain of the counterclockwise neighboring subunit (green; surface representation). Similar rigid-body packing interactions occur between all subunits in the ring and comprise the major subunit-subunit interfaces of the hexamer. **(c)** In this diagram, each $ClpX^{\Delta N}$ subunit is a different color. Four loadable (L) subunits contain a binding site for ATP or ADP (red oval) in a cleft between the large and small AAA+ domains. In two unloadable (U) subunits, a rotation around the intradomain hinge destroys the nucleotide binding site. **(d)** Each rigid-body unit is a different color in this representation, which shows that the $ClpX^{\Delta N}$ ring consists of six rigid-body units connected by six hinges. **(e)** Comparison of individual rigid-body units from nucleotide-free and nucleotide-bound crystal structures of $ClpX^{\Delta N}$ hexamers (pdb codes 3HTE and 3HWS, respectively)[5]. For each rigid-body unit, the large AAA+ domains were structurally aligned (the large domain of subunit A from 3HWS is shown in gray surface representation) and the position of the small AAA+ domain of the rigid-body unit was shown in ribbon representation without alignment (each individual small domain is a different color).

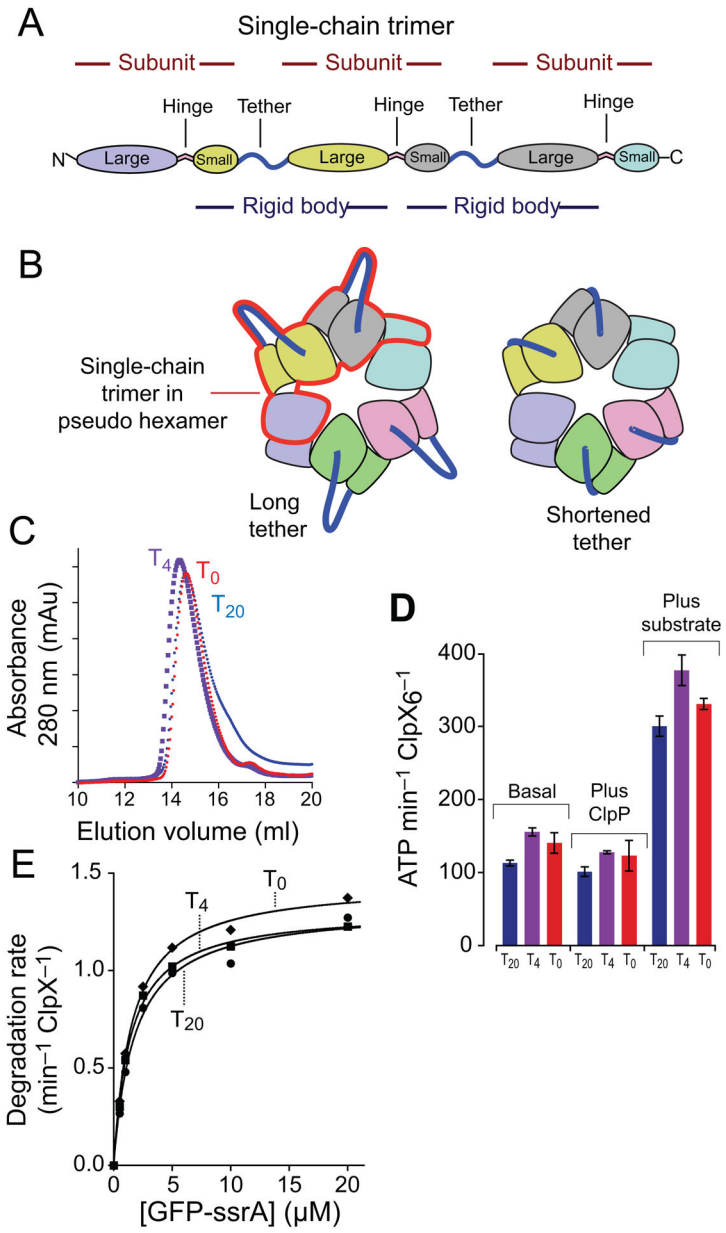

Figure 2.

Fusing rigid-body units with tethers of different lengths. (**a**) A single-chain $ClpX^{\Delta N}$ trimer contains three subunits and two polypeptide linkers that tether adjacent subunits. Each trimer contains two rigid-body units, which are fused by the tethers. **(b)** The position of one single-chain trimer in a pseudo hexamer is marked by the red outline. Shortening the tethers constrains potential movements of the large and small AAA+ domains of the rigid-body unit. **(c)** Single-chain $ClpX^{\Delta N}$ trimers with tethers of 20 residues (T_{20}), 4 residues (T_4), or zero residues (T_0) chromatographed at similar positions on a Superose-6 gel-filtration column (void volume ~8 mL; GE Healthcare). A previous study[15] showed that the T_{20} variant chromatographed identically to non tethered $ClpX^{\Delta N}$ at the position expected for a pseudo hexamer. **(d)** Pseudo hexamers formed from T_0, T_4, or T_{20} single-chain trimers

catalyzed similar basal levels of ATP hydrolysis. This activity was repressed slightly by addition of ClpP and was stimulated markedly by addition of an unfolded protein substrate (carboxymethylated-titin-ssrA)[20]. **(e)** Pseudo hexamers (0.3 μM) formed from T_0, T_4, or T_{20} single-chain $ClpX^{\Delta N}$ trimers supported very similar levels of ClpP (0.9 μM) degradation of GFP-ssrA over a wide range of substrate concentrations. Symbols represent the average of three independent measurements. Lines are non-linear least-squares fits to the Michaelis-Menten equation. Values of K_M and V_{max} are listed in Table 1.

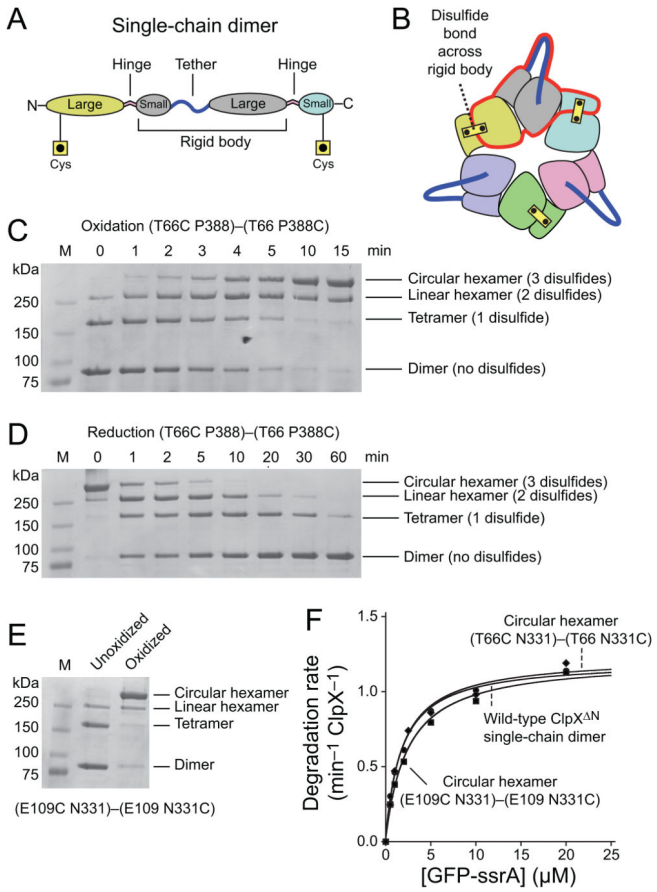

Figure 3.

Stabilizing rigid-body packing between single-chain dimers by disulfide bonds. **(a)** Diagram of a single-chain ClpX$^{\Delta N}$ dimer with cysteines introduced into the large AAA+ domain of the first subunit and the small AAA+ domain of the second subunit. These cysteines were designed to allow disulfide-bond formation within the rigid-body units that form the subunit interfaces between different single-chain ClpX$^{\Delta N}$ dimers in pseudo hexamers. **(b)** Cartoon showing how disulfide bonds across rigid-body units and tethers would covalently connect each subunit in the ClpX$^{\Delta N}$ ring to both neighboring subunits, resulting in topological closure of the ring. **(c)** Non-reducing SDS-PAGE showing the progressive formation of disulfide-bonded species of the (T66C P388)–(T66 P388C) single-chain dimer following initiation of oxidation by addition of copper phenanthroline. The kinetics of formation and disappearance of different species show that the highest band corresponds to the circular hexamer with three disulfide bonds. Bands were visualized by staining with Coomassie Blue. The leftmost lane shows the positions of molecular weight standards. **(d)** The oxidized (T66C P388)–(T66 P388C) single-chain dimer was incubated with 10 mM DTT at 37 °C and the progressive disassembly of disulfide-bonded species was assayed by non-reducing SDS-PAGE. The kinetics of reduction support the pathway: circular hexamer → linear hexamer → linear tetramer → linear dimer. **(e)** Non-reducing SDS-PAGE showing oxidation of (E109C N331)–(E109 N331C) to form the circular hexamer. **(f)** Mixtures containing >90% disulfide-bond circular hexamers of (T66C P388)–(T66 P388C) and

(E109C N331)–(E109 N331C) (0.3 μM) supported similar levels of ClpP (0.9 μM) degradation of GFP-ssrA over a range of substrate concentrations. Symbols are averages of three independent measurements. Lines are fits to the Michaelis-Menten equation, with values of K_M and V_{max} listed in Table 1.

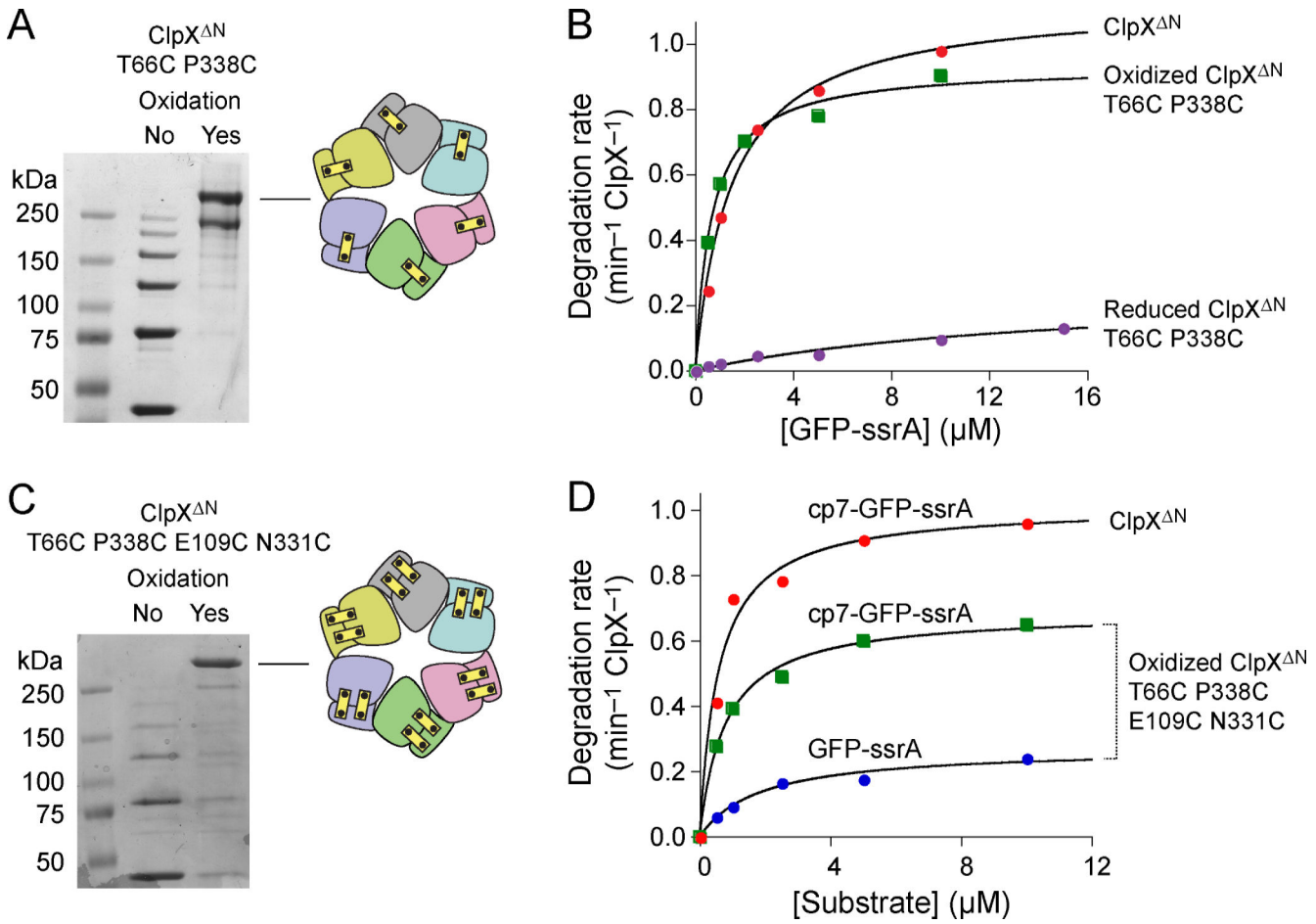

Figure 4.

Closed hexamers with disulfide bonds across all rigid-body subunit interfaces. **(a)** Non-reducing SDS-PAGE showing end-point disulfide-bond formation of T66C P388C ClpX$^{\Delta N}$ after oxidation with copper phenanthroline. **(b)** Michaelis-Menten plots of GFP-ssrA degradation by ClpX$^{\Delta N}$, oxidized T66C P388C ClpX$^{\Delta N}$, or reduced T66C P388C ClpX$^{\Delta N}$ (0.3 μM pseudo hexamer) and ClpP$_{14}$ (0.9 μM). Symbols represent averages of three independent measurements. Table 1 lists values of K_M and V_{max} obtained by curve fitting. **(c)** Non-reducing SDS-PAGE showing end-point disulfide-bond formation of T66C P388C E109C N331C ClpX$^{\Delta N}$ after oxidation with copper phenanthroline. Symbols represent averages of three independent measurements. **(d)** Michaelis-Menten plots of GFP-ssrA or cp7-GFP-ssrA degradation by ClpX$^{\Delta N}$ or oxidized T66C P388C E109C N331C ClpX$^{\Delta N}$ (0.3 μM pseudo hexamer) and ClpP$_{14}$ (0.9 μM). Table 1 lists K_M and V_{max} values.

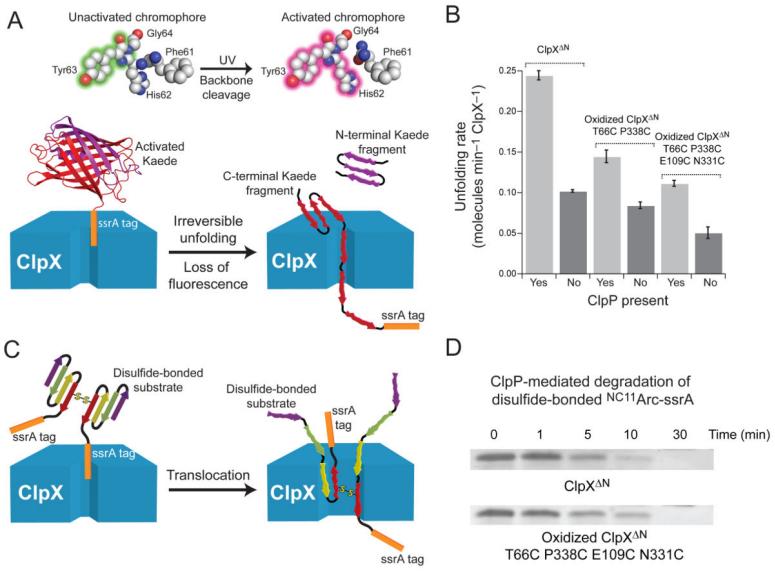

Figure 5.

Unfolding and translocation by $ClpX^{\Delta N}$ circular hexamers. **(a)** Irradiation of Kaede-ssrA with UV light results in photo-cleavage of the polypeptide chain at a single site and a change in fluorescence[24]. Following photo-cleavage, $ClpX^{\Delta N}$ unfolding of Kaede-ssrA is effectively irreversible and eliminates native fluorescence. **(b)** Rates of Kaede-ssrA (10 μM) unfolding were determined for $ClpX^{\Delta N}$, oxidized T66C P388 $ClpX^{\Delta N}$, and oxidized T66C P388C E109C N331C $ClpX^{\Delta N}$ (0.3 μM pseudo hexamer) with or without $ClpP_{14}$ (0.9 μM). Values are averages of 3 independent experiments ± 1 standard deviation. **(c)** ClpXP degradation of disulfide-bonded substrates requires concurrent translocation of multiple polypeptide chains. **(d)** Non-reducing SDS-PAGE showing that degradation of disulfide-bonded ^{N11C}Arc-ssrA (10 μM) by $ClpX^{\Delta N}$ or by oxidized T66C P388C E109C N331C $ClpX^{\Delta N}$ (0.3 μM hexamer) and $ClpP_{14}$ (0.9 μM) occurs with comparable kinetics.

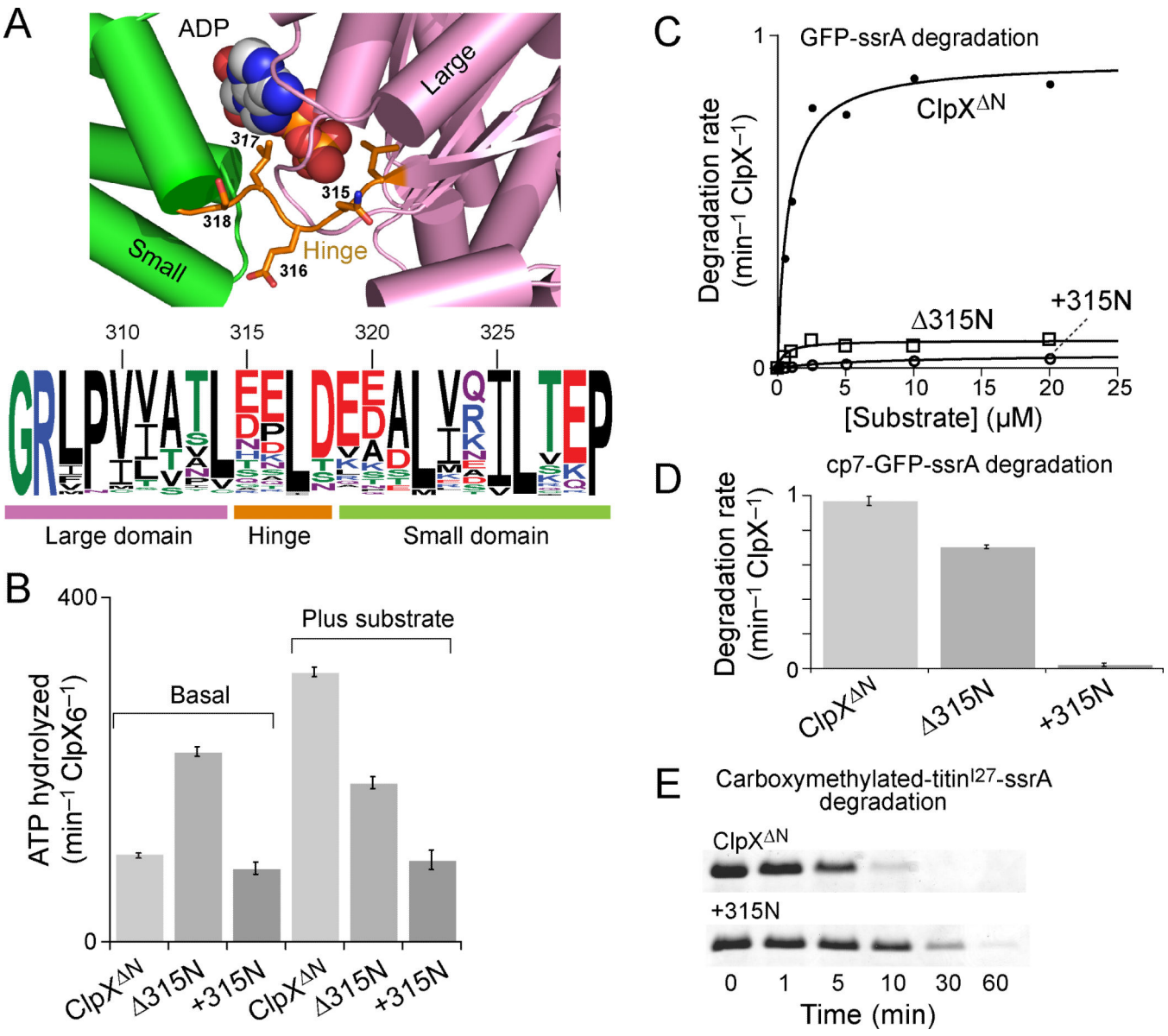

Figure 6.

ClpX hinge mutations uncouple ATP hydrolysis and substrate unfolding. **(a)** The upper panel shows that the nucleotide-binding site in a loadable ClpX subunit (pdb code 3HWS, chain A)[5] lies in a cleft formed by the large AAA+ domain, the hinge, and the small AAA+ domain. In *E. coli* ClpX, the hinge sequence is Asn315-Glu316-Leu317-Ser318. The lower panel is a histogram of sequence conservation from an alignment of >200 ClpX orthologs and was prepared using WebLogo[39]. The length of the hinge is highly conserved, but only Leu317, which contacts the nucleotide base, shows strong sequence conservation. Numbers represent residue positions in *E. coli* ClpX. **(b)** Rates of ATP hydrolysis by 0.3 μM $ClpX^{\Delta N}$ hexamer, Δ315N $ClpX^{\Delta N}$ hexamer, or +315N $ClpX^{\Delta N}$ hexamer were assayed in the absence or presence of carboxymethylated-$titin^{I27}$-ssrA (20 μM). Values are averages of 3 independent experiments ± 1 standard deviation. **(c)** Michaelis-Menten plots of the rate of

degradation of different concentrations of GFP-ssrA in the presence of 0.9 μM $ClpP_{14}$ and 0.3 μM $ClpX^{\Delta N}$ hexamer (K_M = 0.8 μM; V_{max} = 0.92^{-1} min $ClpX_6^{-1}$), Δ315N $ClpX^{\Delta N}$ hexamer (K_M = 0.6 μM; V_{max} = 0.08 min^{-1} $ClpX_6^{-1}$) or +315N $ClpX^{\Delta N}$ hexamer (K_M = 8 μM; V_{max} = 0.04 min^{-1} $ClpX_6^{-1}$). **(d)** Rates of degradation of 10 μM cp7-GFP-ssrA in the presence of 0.9 μM $ClpP_{14}$ and 0.3 μM $ClpX^{\Delta N}$ hexamer, Δ315N $ClpX^{\Delta N}$ hexamer, or +315N $ClpX^{\Delta N}$ hexamer. Values are averages of 3 independent experiments ± 1 standard deviation.

(**e**) SDS-PAGE assay of the degradation of an unfolded substrate, carboxymethylated-$titin^{I27}$-ssrA (20 μM), by 0.9 μM $ClpP_{14}$ and either 0.3 μM $ClpX^{\Delta N}$ hexamer or +315N $ClpX^{\Delta N}$ hexamer.

Table 1

Steady-state kinetic parameters for ClpXP degradation of GFP substrates.

	GFP-ssrA substrate	
ClpX variant	**V_{max} (min^{-1} $ClpX_6^{-1}$)**	**K_M (μM)**
$ClpX^{\Delta N}$-T_{20}-$ClpX^{\Delta N}$-T_{20}-$ClpX^{\Delta N}$	1.3	1.8
$ClpX^{\Delta N}$-T_4-$ClpX^{\Delta N}$-T_4 -$ClpX^{\Delta N}$	1.3	1.4
$ClpX^{\Delta N}$ -T_0-$ClpX^{\Delta N}$-T_0-$ClpX^{\Delta N}$	1.5	1.6
$ClpX^{\Delta N}$ -T_{20}-$ClpX^{\Delta N}$	1.2	1.6
oxidized $ClpX^{\Delta N}$(T66C)-T_{20}-$ClpX^{\Delta N}$(P388C) [(a)]	1.2	1.9
oxidized $ClpX^{\Delta N}$(E109C)-T_{20}-$ClpX^{\Delta N}$(N331C) [(a)]	1.2	2.7
$ClpX^{\Delta N}$	1.1	1.5
oxidized T66C P388C $ClpX^{\Delta N}$ [(b)]	0.9	0.7
oxidized T66C P388C E109C N331C $ClpX^{\Delta N}$ [(a)]	0.27	1.8
	cp7-GFP-ssrA substrate	
$ClpX^{\Delta N}$	1.0	0.6
oxidized T66C P388C E109C N331C $ClpX^{\Delta N}$ [(a)]	0.7	0.8

For oxidized enzymes, >90% (a) or > 75% (b) of the protein was present as the covalently closed circular hexamer as judged by SDS-PAGE.